Nanoconfinement Allows a Less Active Cascade Catalyst to Produce More C_{2+} Products in Electrochemical CO_2 Reduction

Samuel V. Somerville,[†] Peter B. O'Mara,[†] Tania M. Benedetti,[†#] Soshan Cheong,[§] Wolfgang Schuhmann,[‡] Richard D. Tilley,*[,§,†] J. Justin Gooding*[,†]

† School of Chemistry and Australian Centre for NanoMedicine, University of New South Wales, Sydney 2052, Australia

‡ Analytical Chemistry - Center for Electrochemical Sciences (CES), Faculty of Chemistry and Biochemistry, Ruhr-Universitat Bochum, Universitatsstraße 150, D-44780 Bochum, Germany

§ Electron Microscope Unit, Mark Wainwright Analytical Centre, University of New South Wales, Sydney 2052, Australia

Supporting Information

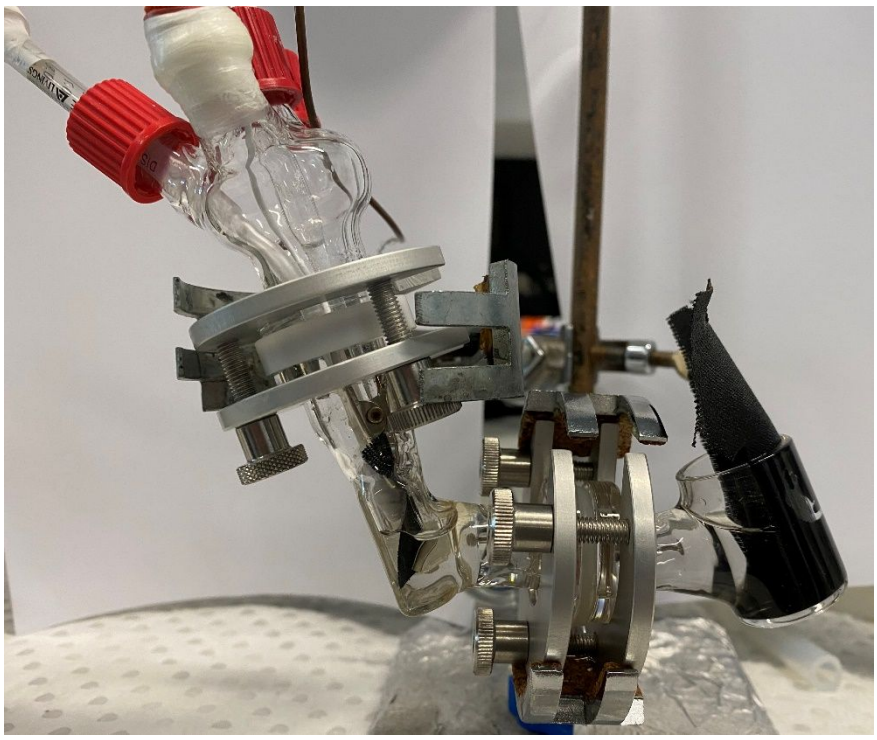

Figure S1: Photograph of the custom low volume H-cell used for all electrochemical experiments. The cathodic and anodic compartment separated by a anion exchange membrane. The cathodic compartment (left) containing the gas dispersion tube, the carbon cloth working electrode, and the reference electrode with Luggin capillary. The anodic compartment containing the Ir nanoparticle loaded counter electrode.

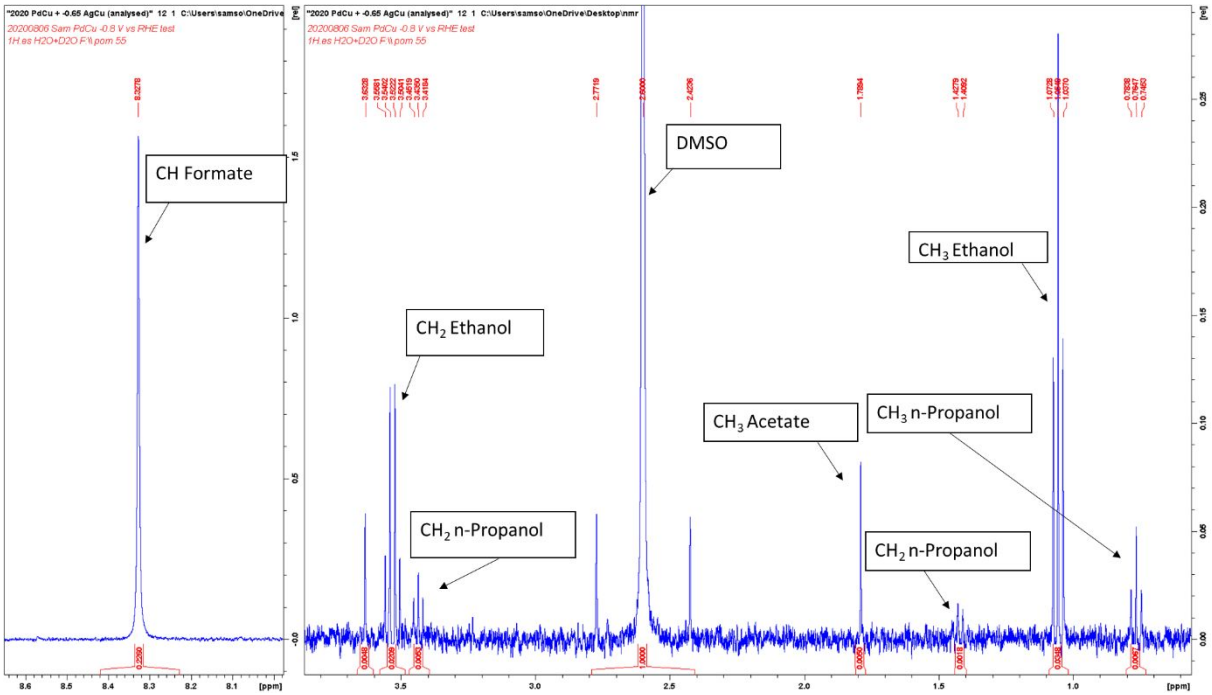

Figure S2: 400 MHz ^{1}H NMR spectrum of liquid products obtained during one-hour electrochemical CO_2RR experiment on the PdCu nanozyme at -0.8 V vs RHE in 0.1 M $KHCO_3$.

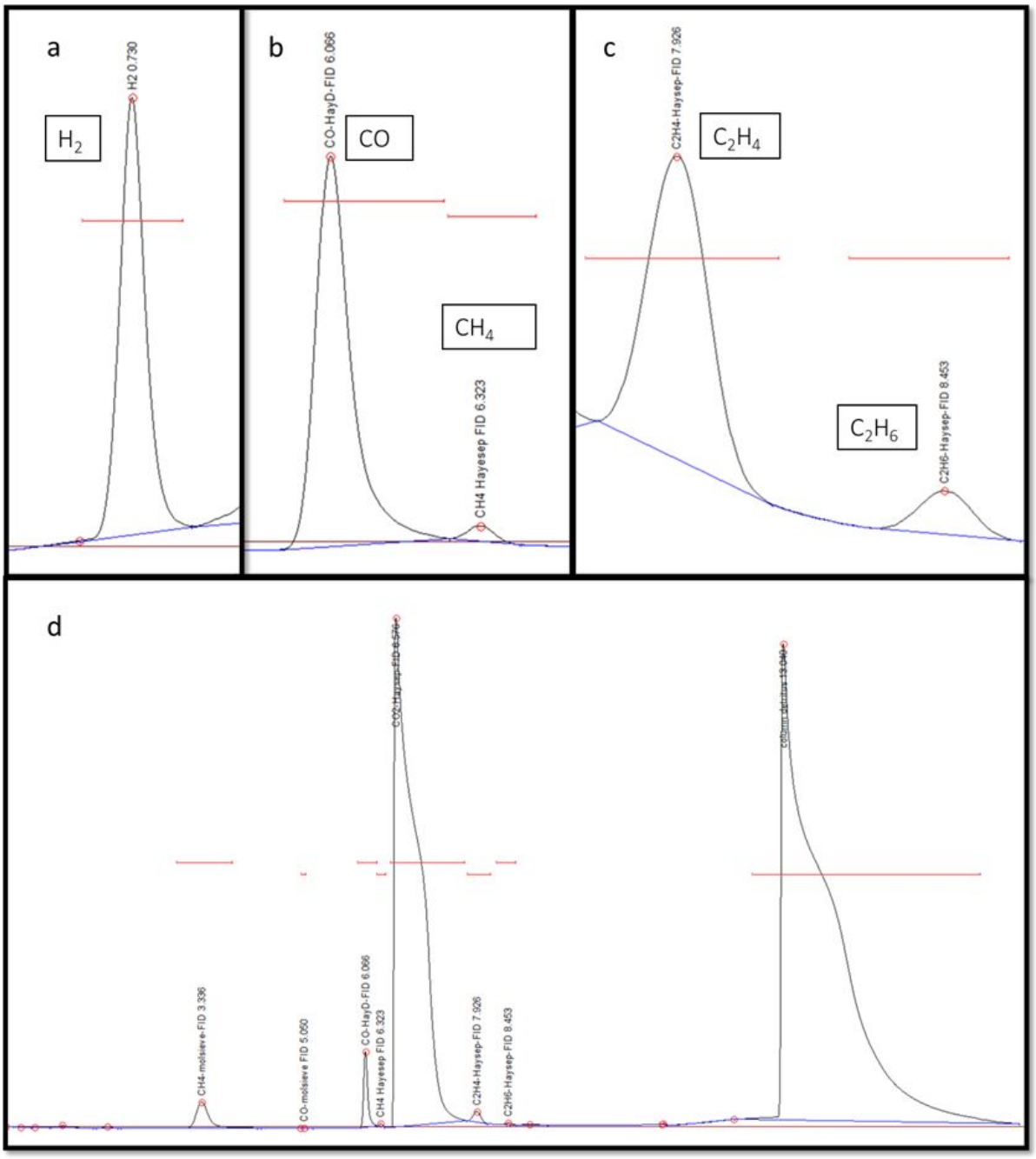

Figure S3: GC output for the third injection of the PdCu nanozyme under an applied potential of -0.8 V vs RHE in CO_2 saturated $KHCO_3$. (a) TCD chromatograph highlighting H_2 peak and sectiosn of FID chromatograph highlighting (b) CO and methane, (c), ethene and ethane peaks and retention time, (d) shows the full FID chromatograph.

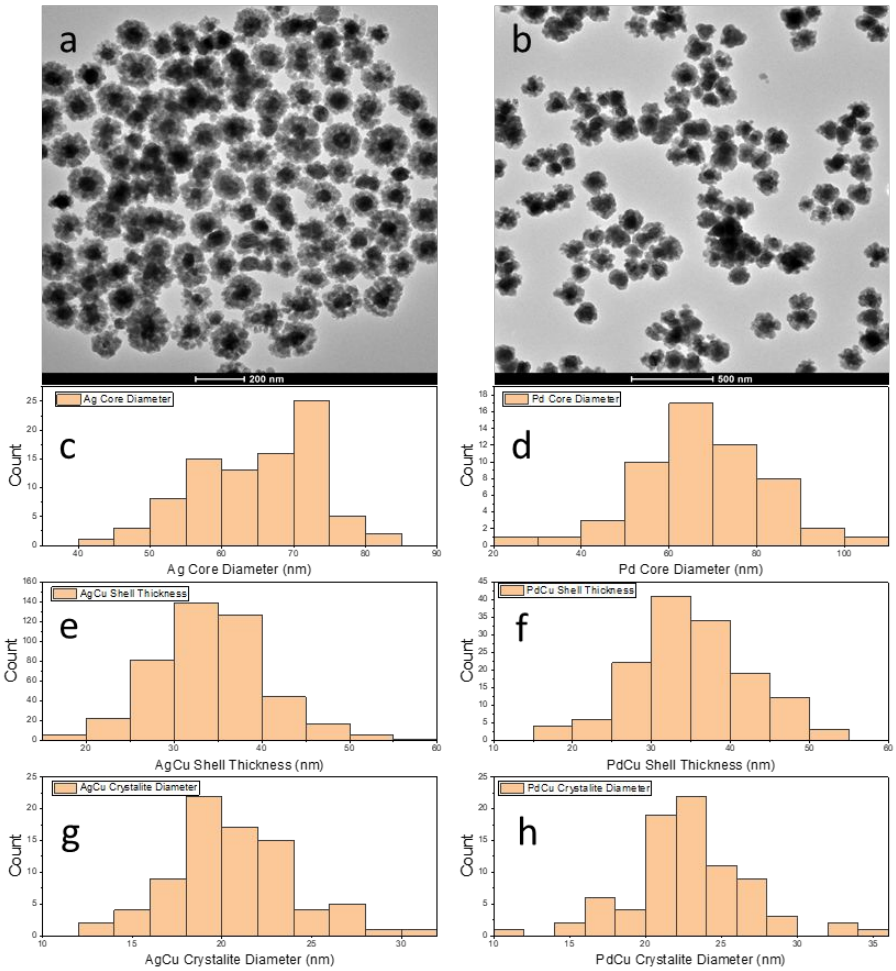

Figure S4: Nanoparticle characterisation: (a) low resolution TEM of AgCu nanozymes, (b) low resolution TEM of PdCu nanozymes, (c) histograms of Ag core diameter, (d) Pd core diameter, (e) AgCu shell thickness, (f) PdCu shell thickness, (g) AgCu Cu crystallite size, (h) PdCu Cu crystallite size.

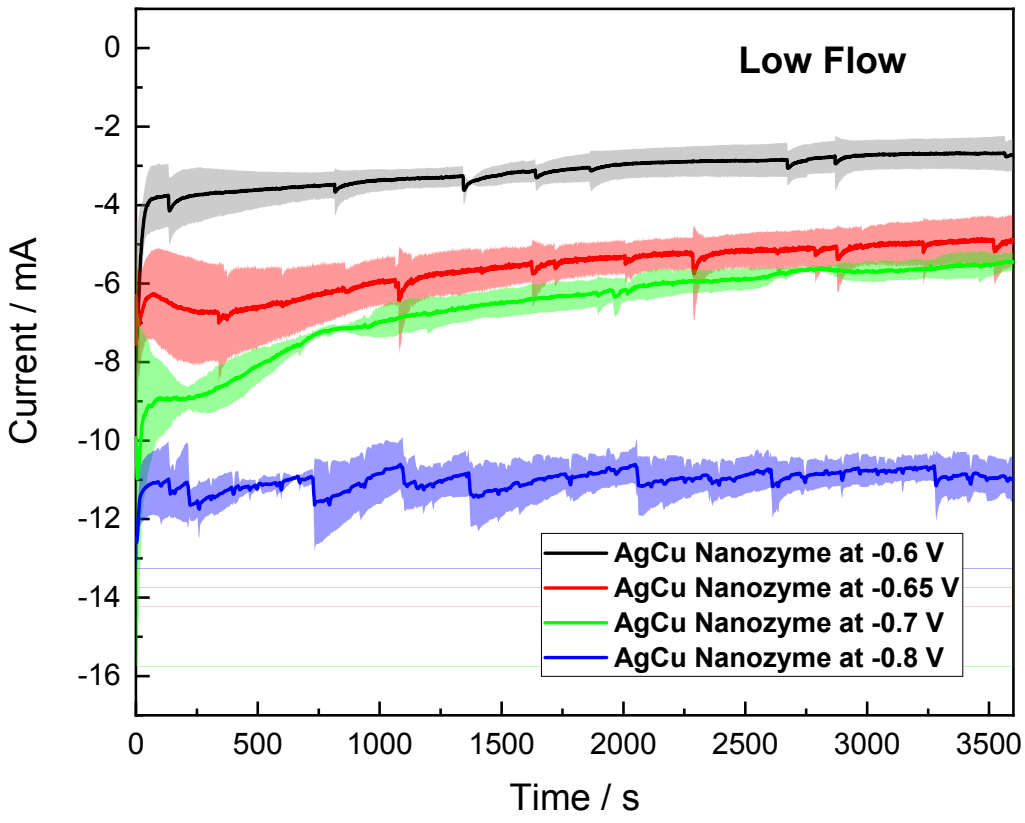

Figure S5: Chronoamperogram of the AgCu nanozyme catalysts during CO_2 reduction reaction under a 5 mL/min CO_2 flow rate. Chronoamperograms were recorded for 1 h at different applied potentials vs. RHE.

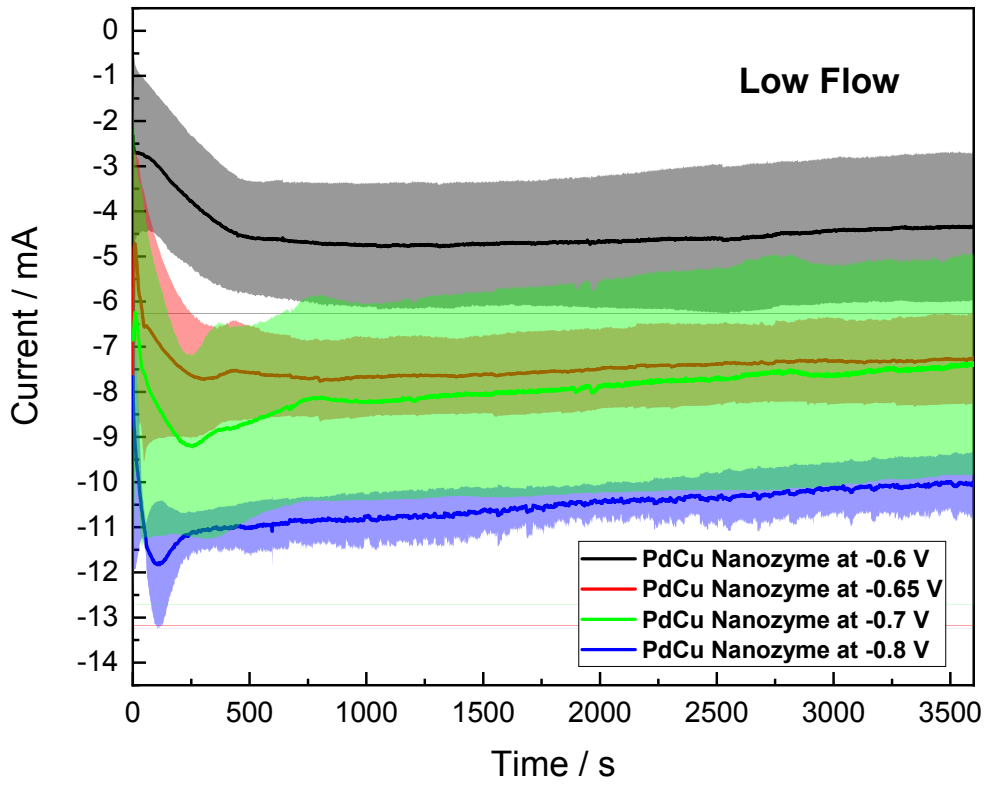

Figure S6: Chronoamperogram of the PdCu nanozyme catalysts during CO_2 reduction reaction under a 5 mL/min CO_2 flow rate. Chronoamperograms were recorded for 1 h at different applied potentials vs. RHE.

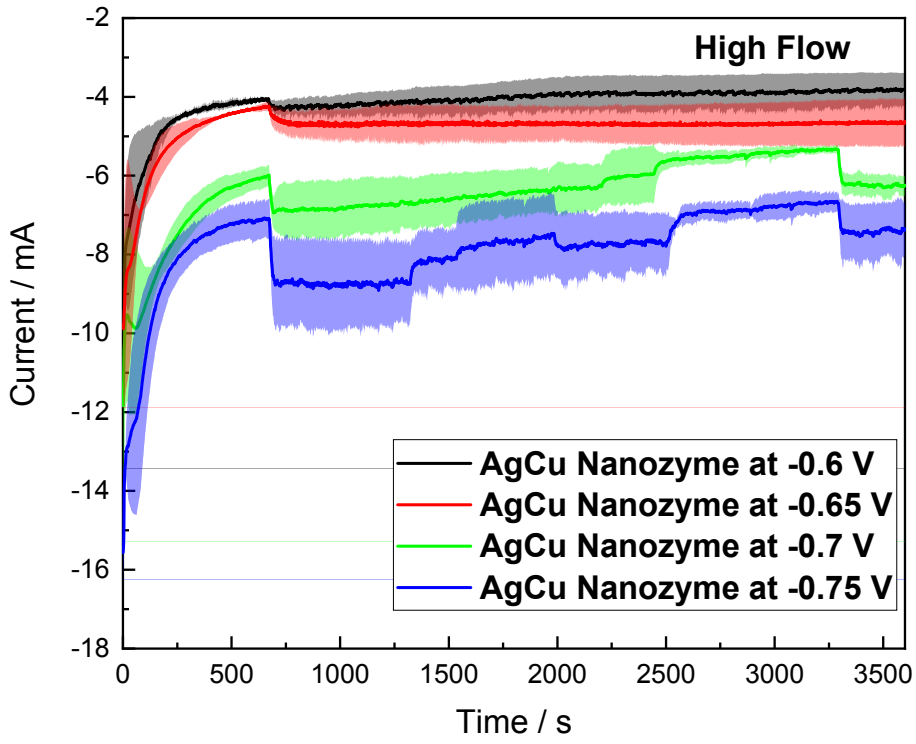

Figure S7: Chronoamperogram of the AgCu nanozyme catalysts during CO_2 reduction reaction under a 20 mL/min CO_2 flow rate. Chronoamperograms were recorded for 1 h at different applied potentials vs. RHE.

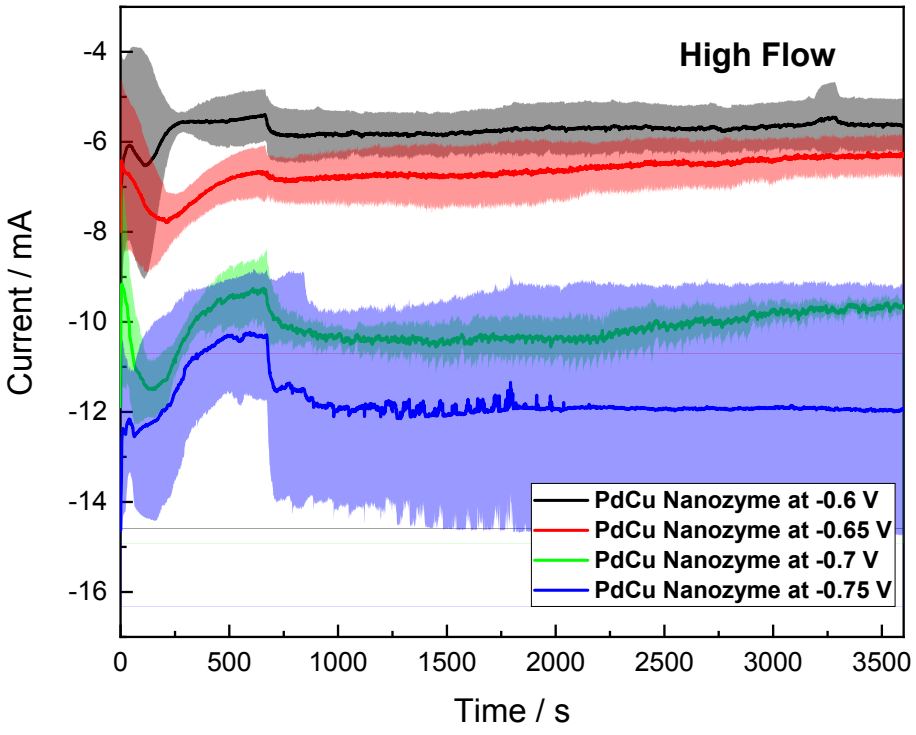

Figure S8: Chronoamperogram of the PdCu nanozyme catalysts during CO_2 reduction reaction under a 20 mL/min CO_2 flow rate. Chronoamperograms were recorded for 1 h at different applied potentials vs. RHE.

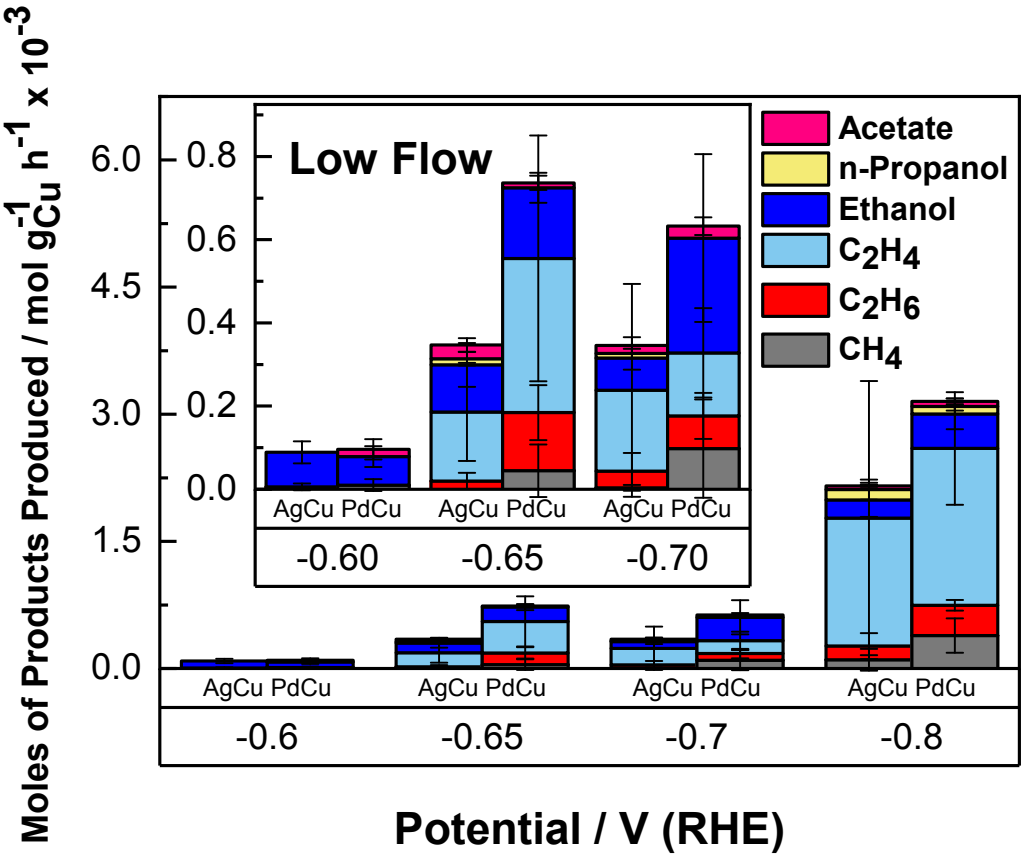

Figure S9: Moles of products produced per gram of Cu at -0.60, -0.65, -0.70, -0.80 V vs RHE a one-hour electrochemical experiment in 0.1 M $KHCO_3$ at 5 mL/min CO_2 flow rate for the AgCu and PdCu nanozymes.

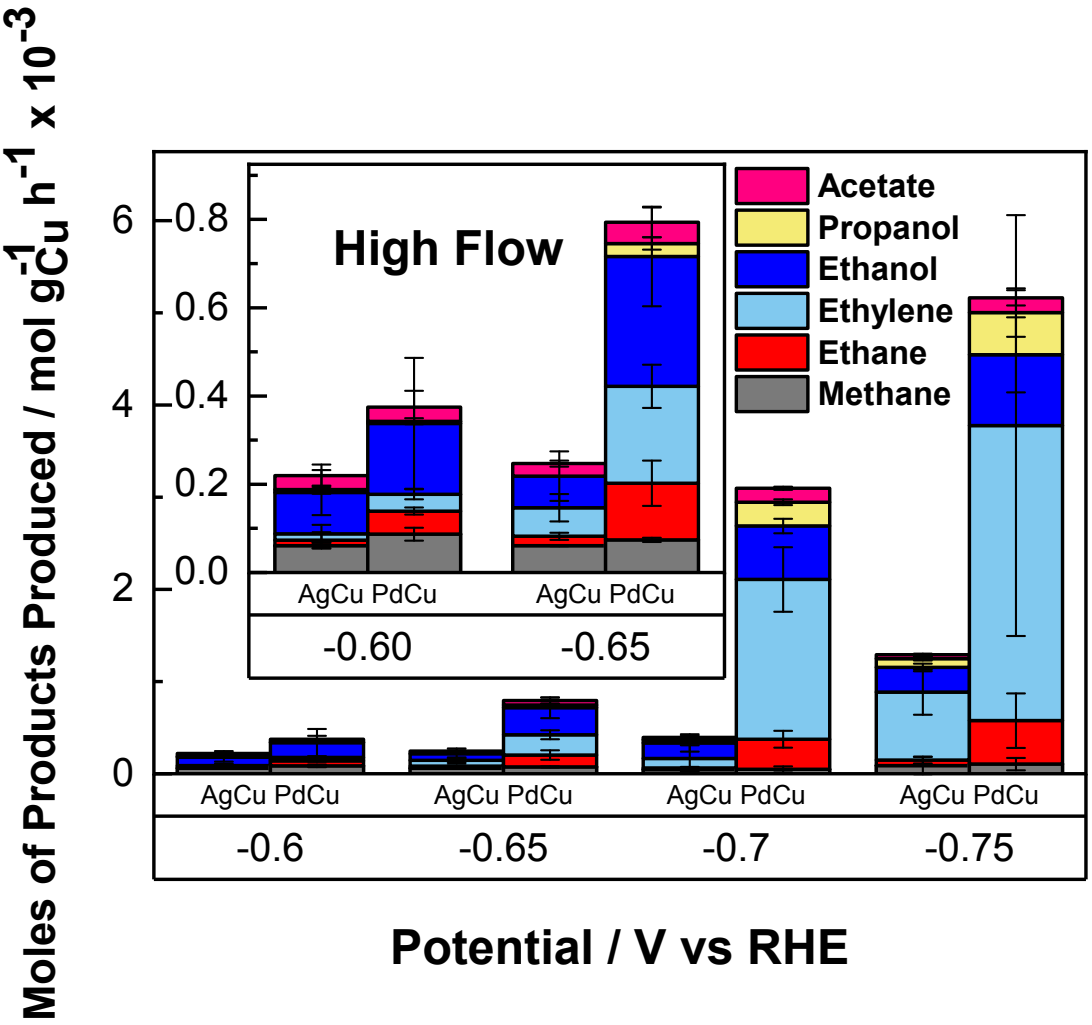

Figure S10: Moles of products produced per gram of Cu at -0.60, -0.65, -0.70, -0.75 V vs RHE a one-hour electrochemical experiment in 0.1 M $KHCO_3$ at 20 mL/min CO_2 flow rate for the AgCu and PdCu nanozymes.

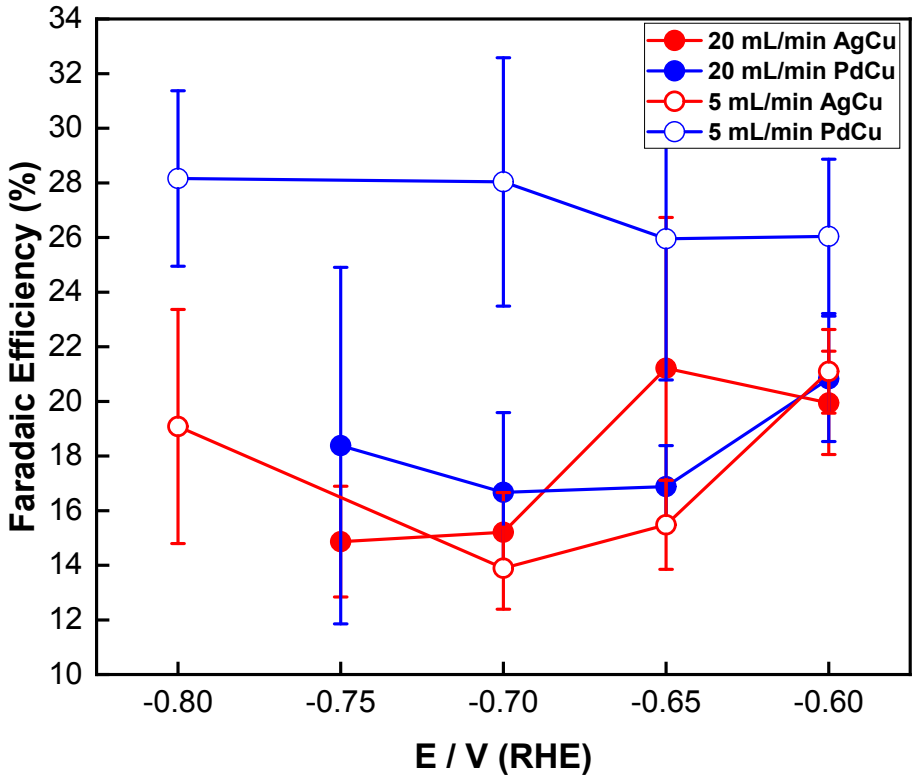

Figure S11: Faradaic efficiency for the production of H_2 at -0.60, -0.65, -0.70, 0.75 -0.80 V vs RHE in a one-hour electrochemical experiment in 0.1 M $KHCO_3$ with 20 mL/min (filled), 5 mL/min CO_2 flow rate (hollow), AgCu (red), and PdCu (blue).

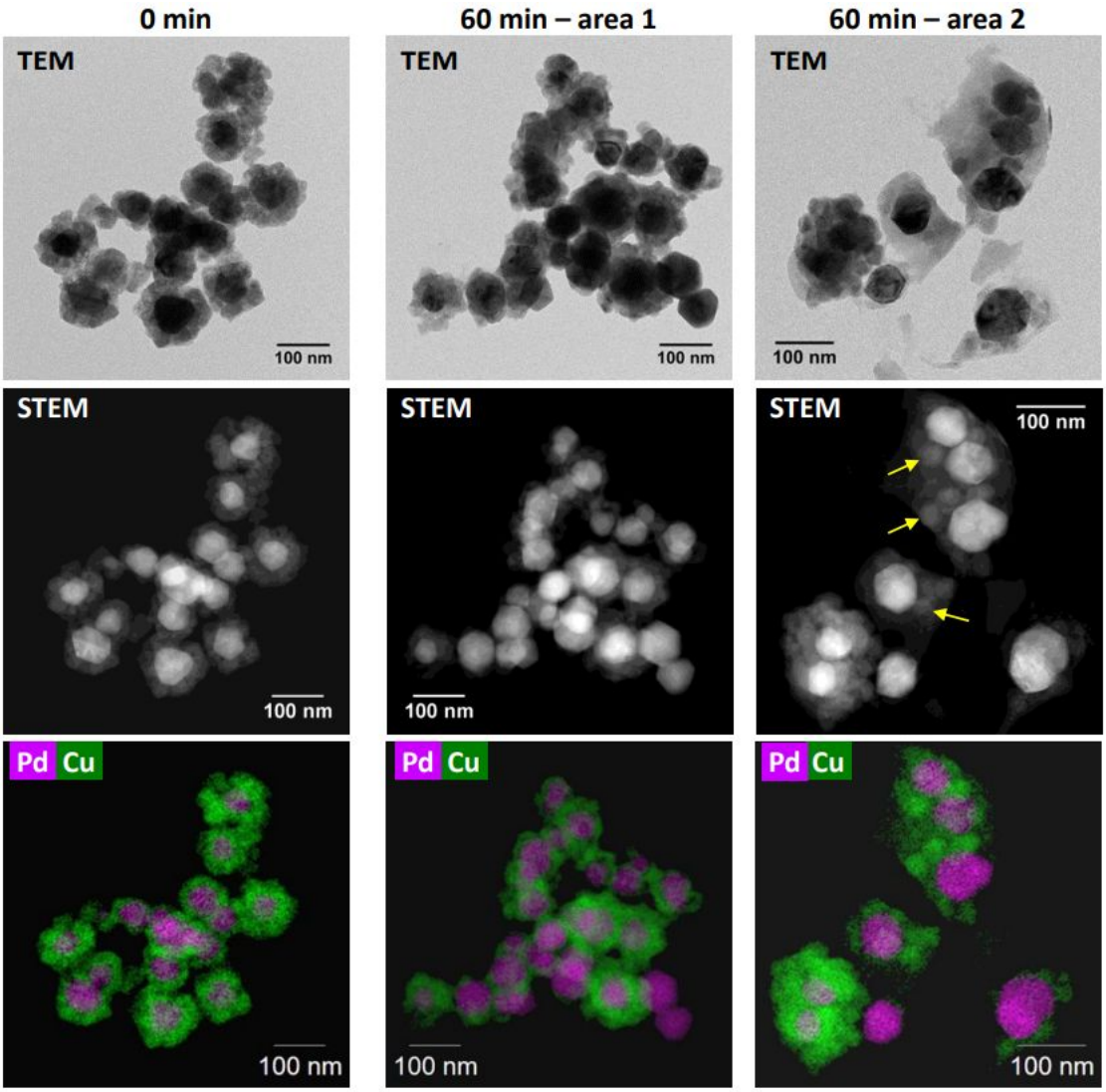

Figure S12: HRTEM, STEM and EDX analysis of the pre-catalysis PdCu nanozymes and two areas of post-catalysis particles. Yellow arrows depict sintered CuO regions surrounding the Pd cores, with crystalline CuO nanoparticles embedded within an amorphous CuO matrix.

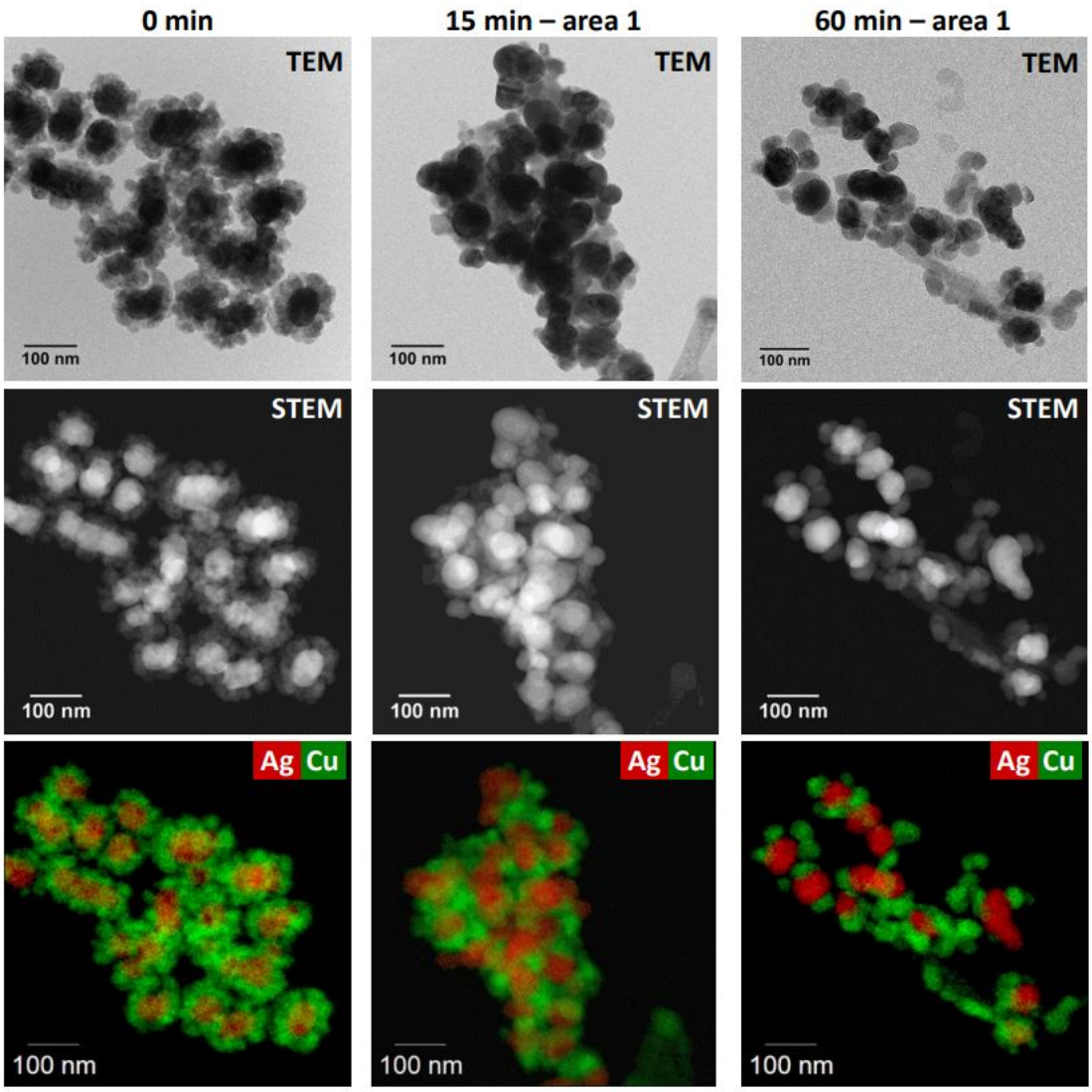

Figure S13: HRTEM, STEM and EDX analysis of the AgCu nanozymes at 0, 15 and 60 min depicting the change from pristine core-shell structure at 0 mins to the onset of shell destruction at 15 min and the complete disintegration of the structure at 60 min.

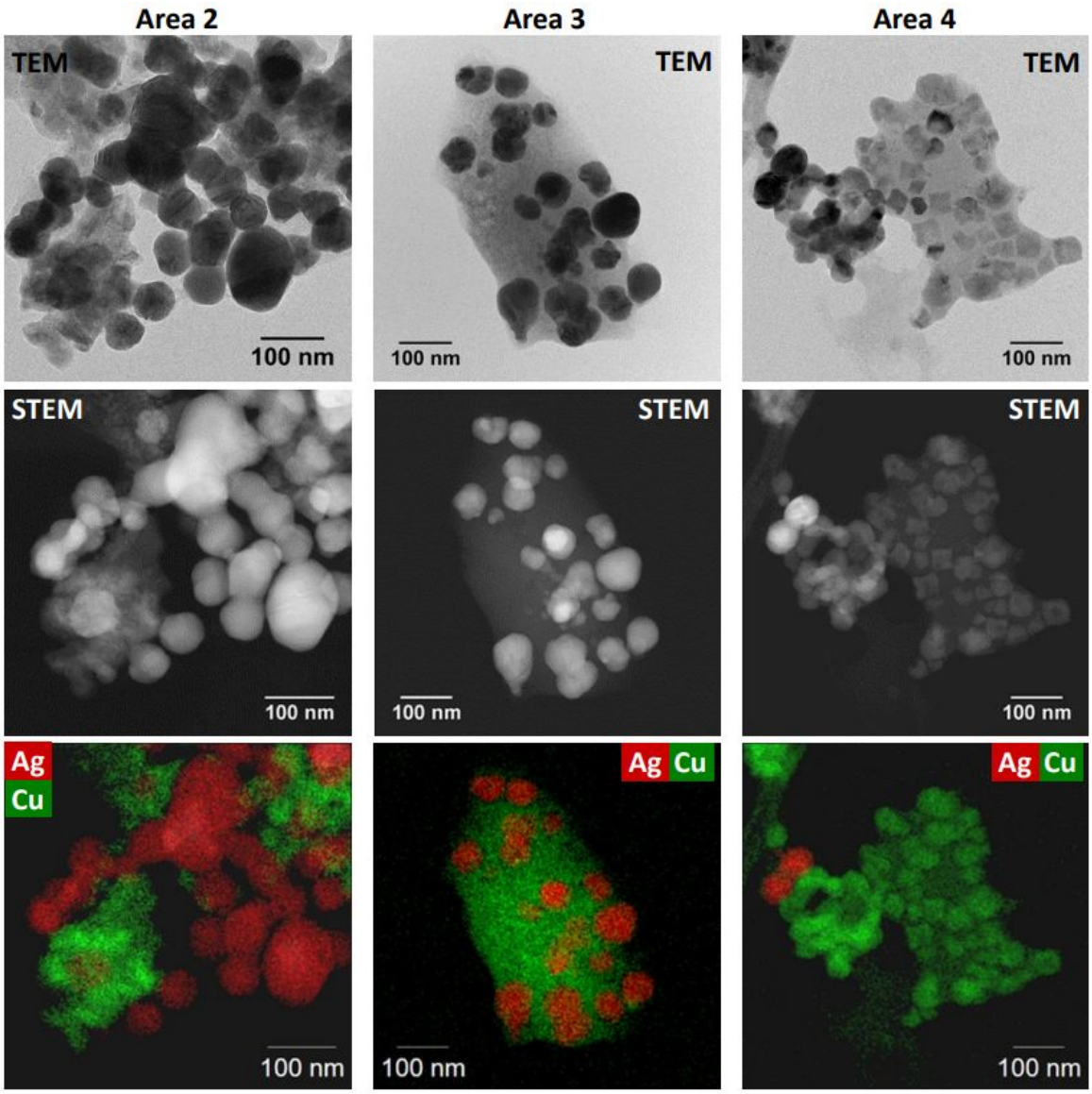

Figure S14: HRTEM, STEM and EDX analysis of 3 regions of the AgCu nanozyme sample after 15 min of catalysis highlighting the polydispersity of structures arising from particle destruction with some CuO forming large amorphous regions and others forming crystallites.

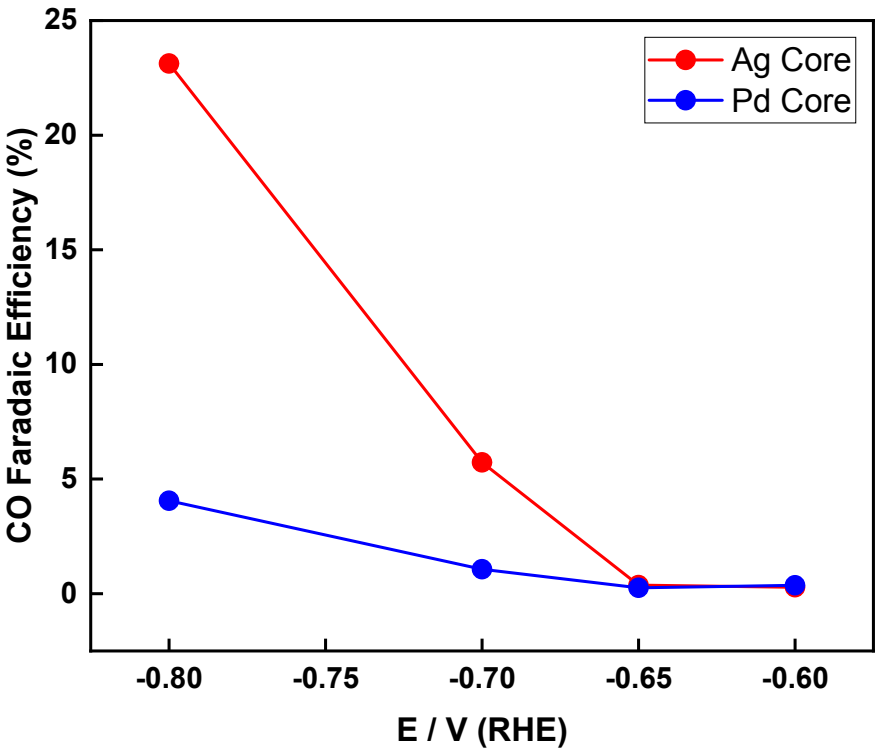

Figure S15: Faradaic efficiency for CO at -0.60, -0.65, -0.70, and -0.80 V vs RHE in a one-hour electrochemical experiment in 0.1 M $KHCO_3$ with AgCu (red), and PdCu (blue).

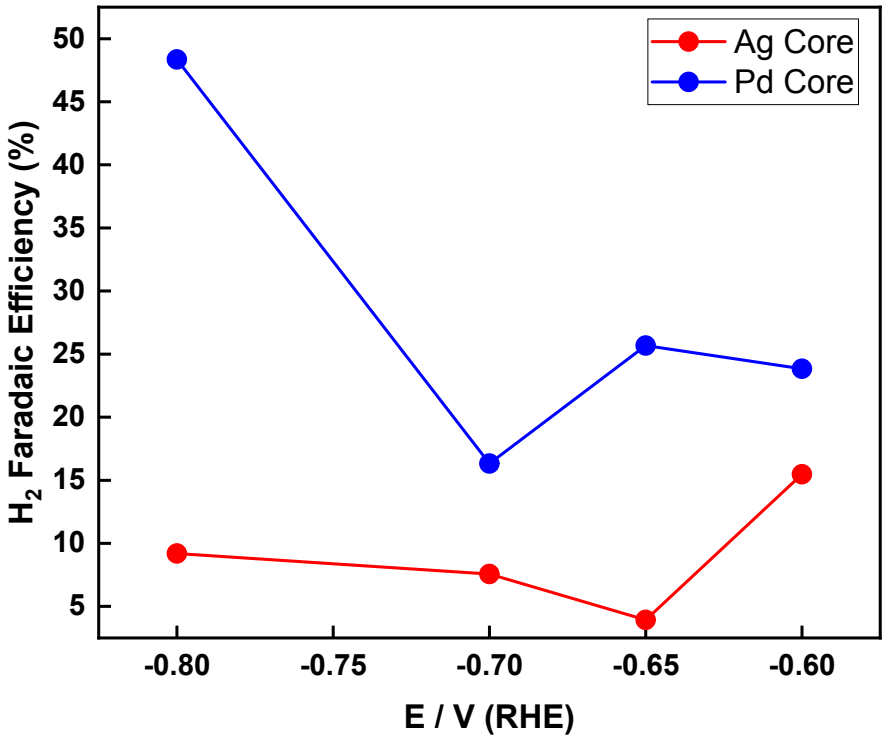

Figure S16: Faradaic efficiency for H_2 at -0.60, -0.65, -0.70, and -0.80 V vs RHE in a one-hour electrochemical experiment in 0.1 M $KHCO_3$ with AgCu (red), and PdCu (blue).

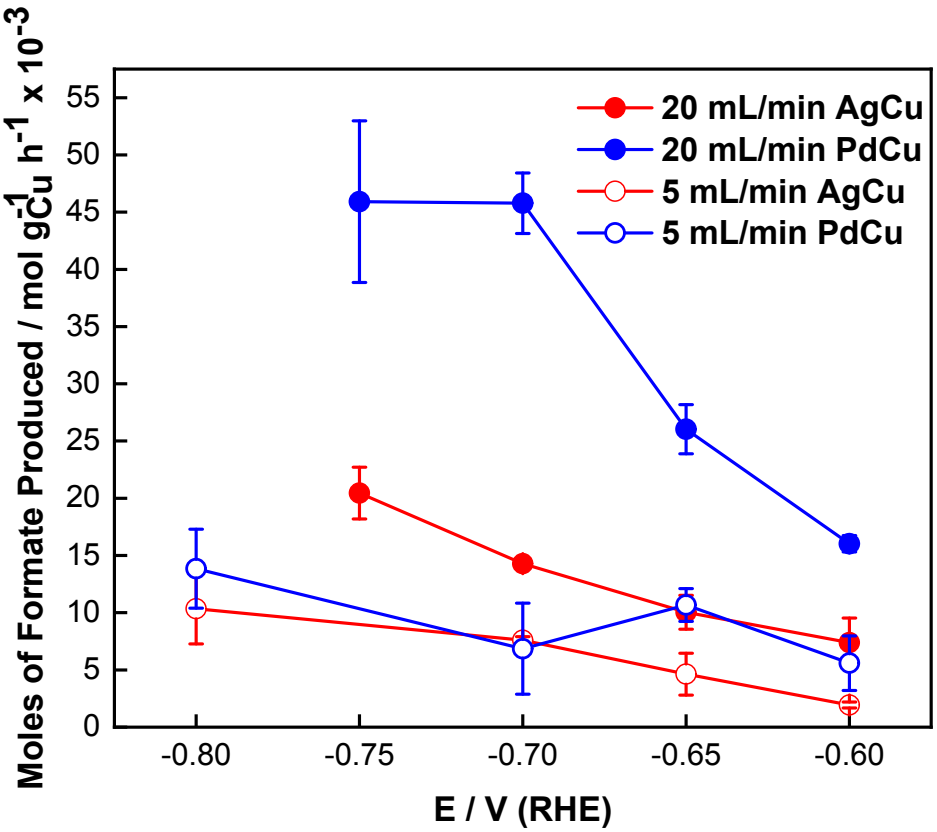

Figure S17: Moles of formate produced per gram of Cu at -0.60, -0.65, -0.70, -0.75, -0.80 V vs RHE in a one-hour electrochemical experiment in 0.1 M $KHCO_3$ with 20 mL/min (filled), 5 mL/min CO_2 flow rate (hollow), AgCu (red), and PdCu (blue).

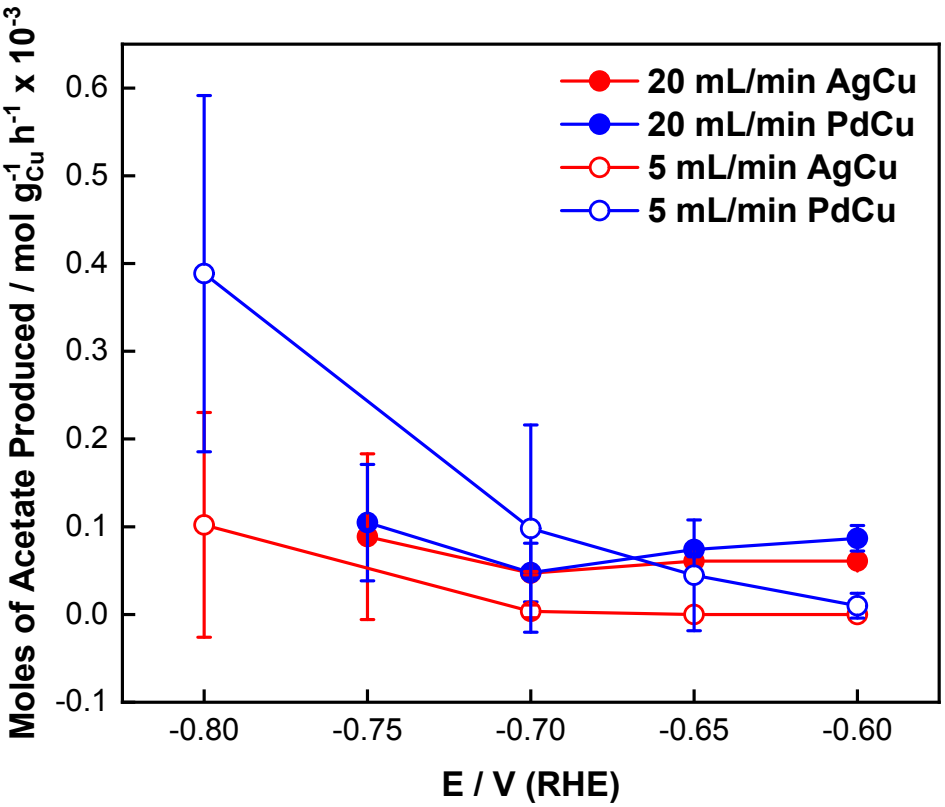

Figure S18: Moles of methane produced per gram of Cu at -0.60, -0.65, -0.70, -0.75, -0.80 V vs RHE in a one-hour electrochemical experiment in 0.1 M $KHCO_3$ with 20 mL/min (filled), 5 mL/min CO_2 flow rate (hollow), AgCu (red), and PdCu (blue).

ow), AgCu (red), and PdCu (blue).

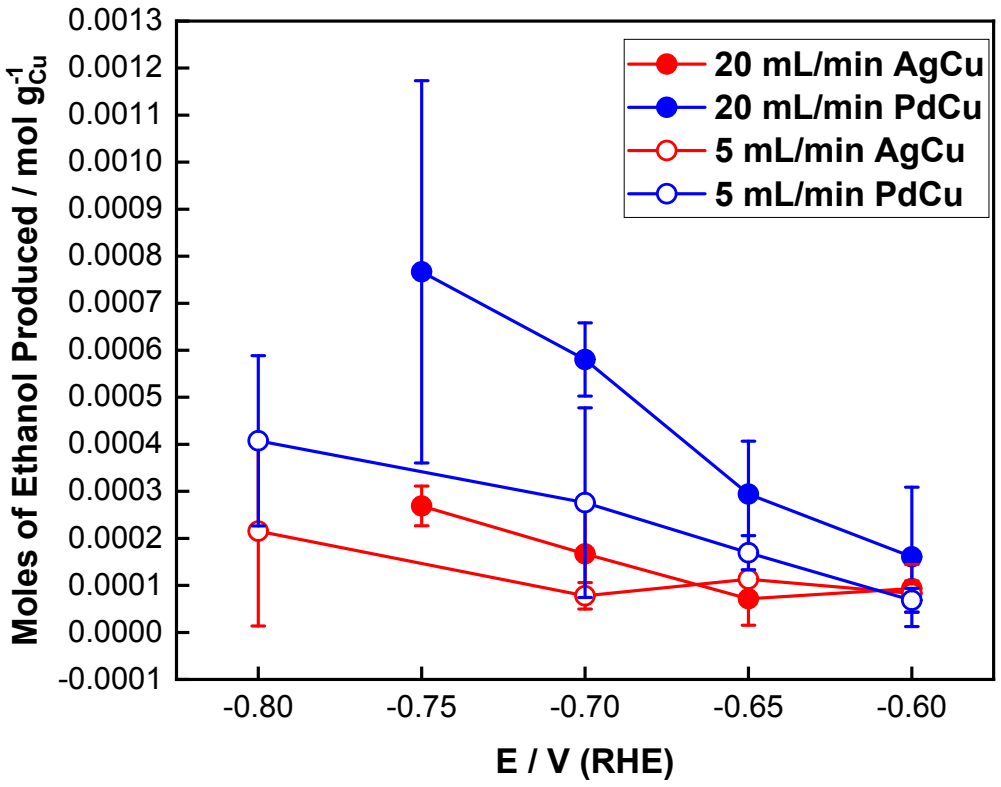

Figure S19: Moles of ethanol produced per gram of Cu at -0.60, -0.65, -0.70, -0.75, -0.80 V vs RHE in a one-hour electrochemical experiment in 0.1 M $KHCO_3$ with 20 mL/min (red), 5 mL/min (blue), AgCu (filled), and PdCu (hollow).

	AgCu		PdCu	
	Ag	Cu	Pd	Cu
Sample 1 / mg L^{-1}	35.9	31.7	20.5	23.1
Sample 2 / mg L^{-1}	31.5	27.9	21.6	25.4
Sample 3 / mg L^{-1}	37.9	33.6	22.1	24.2
average / mg L^{-1}	35.1	31.1	21.4	24.3
standard deviation / mg L^{-1}	2.7	2.4	0.9	0.9
concentration of metal in ink / mg mL^{-1}	3.51	3.11	2.21	2.41
amount of metal on electrode / mg	0.84	0.75	0.53	0.59
amount of Core metal + Cu on electrode / mg	1.59		1.12	

Table S1: The raw data from inductively coupled plasma optical emission spectroscopy (ICP-OES), and the process to derive information on the loading of the nanoparticles. Samples were prepared by dissolving 100 µL of 7.5 mg·mL^{-1} catalyst ink in 1.0 mL of concentrated HNO_3 and heated at 80 °C for 1 h, then diluted to 10 mL with water.

(1) Chen, B.; Jiao, X.; Chen, D. Size-Controlled and Size-Designed Synthesis of Nano/Submicrometer Ag Particles. *Cryst. Growth Des.* **2010**, *10* (8), 3378–3386.

https://doi.org/10.1021/cg901497p.

(2) Chen, H.; Wei, G.; Ispas, A.; Hickey, S. G.; Eychmüller, A. Synthesis of Palladium Nanoparticles and Their Applications for Surface-Enhanced Raman Scattering and Electrocatalysis. *J. Phys. Chem. C* **2010**, *114* (50), 21976–21981. https://doi.org/10.1021/jp106623y.

(3) Zhang, L.; Jing, H.; Boisvert, G.; He, J. Z.; Wang, H. Geometry Control and Optical Tunability of Metal-Cuprous Oxide Core-Shell Nanoparticles. *ACS Nano* **2012**, *6* (4), 3514–3527. https://doi.org/10.1021/nn300546w.